Recent Belle results

Dmitri Liventsev[1]

[1]KEK, 1-1 Oho, Tsukuba-shi, Ibaraki-ken, 305-0801 Japan

We review the recent results from the Belle experiment: search for new physics in $B \to \tau\nu$ and related decays, study of charged bottomonium-like states Z_b and measurement of the parameters of the Cabibbo-Kobayashi-Maskawa matrix in $B^0 \to \pi^+\pi^-$ and $B^0 \to \rho^0\rho^0$ decays.

1 $B \to \tau\nu$ and related results

1.1 Introduction

The purely leptonic decay $B \to \tau\nu$ is of high interest since it provides a unique opportunity to test the Standard Model (SM) and search for new physics beyond the SM. In the absence of new physics, this measurement provides a direct experimental determination of the product of the B meson decay constant and the CKM matrix element $f_B|V_{ub}|$. Physics beyond the SM, however, could significantly suppress or enhance $\mathcal{B}(B \to \tau\nu)$ via exchange of a new charged particle, *e.g.* a charged Higgs boson from two-Higgs doublet models (2HDM) [1, 2]. Leptonic $B \to \ell\nu$, $\ell = e, \mu$ and semileptonic $B \to D^{(*)}\tau\nu$ decays are also sensitive to such exchange [3]. Here recent results obtained at the B-factories are reviewed. The comparison between the experimental results and the SM predictions is shown. The constraints on the Type II 2HDM are reported.

1.2 $B \to \tau\nu$

It is challenging to identify the $B \to \tau\nu$ decay experimentally, since it includes multiple neutrinos in the final state. At the e^+e^- B-factories a B meson pair is generated from the process $e^+e^- \to \Upsilon(4S) \to B\bar{B}$ and we can reconstruct one of the B mesons ("$B_{\rm tag}$") to identify the decay of the other B meson ("$B_{\rm sig}$"). Two independent types of the B meson decays may be used for reconstruction of $B_{\rm tag}$: hadronic decays such as $B^- \to D^0\pi^-$ ("hadronic tag") and semileptonic decays such as $B^- \to D^0\ell^-\nu$, $\ell = e, \mu$ ("semileptonic tag"). The efficiency for reconstructing $B_{\rm tag}$ is higher for the semileptonic tag, while the purity is higher for the hadronic tag.

The first evidence for $B \to \tau\nu$ was reported by the Belle collaboration using hadronic tag and a data sample corresponding to 449×10^6 $B\bar{B}$ events [4]. This was followed by a measurement using semileptonic tag and a data sample corresponding to 657×10^6 $B\bar{B}$ events [5]. The branching ratio obtained by the semileptonic tag analysis is $\mathcal{B}(B \to \tau\nu) = [1.54^{+0.38}_{-0.37}(stat)^{+0.29}_{-0.31}(syst)] \times 10^{-4}$, with a significance of 3.6σ. The hadronic tag result has been updated using Belle final data sample corresponding to 772×10^6 $B\bar{B}$ events [6]. By employing a neural network-based method for the hadronic tag [7] and a two-dimensional fit for the signal extraction, along with a larger data sample, both statistical and systematic precision is significantly improved. The branching ratio is obtained to be $\mathcal{B}(B \to \tau\nu) = [0.72^{+0.27}_{-0.25}(stat) \pm 0.11(syst)] \times 10^{-4}$, with significance of 3.0σ. Results of the fit are shown in Fig. 1. Combining the semileptonic tag and hadronic tag results and taking into account all the correlated systematic uncertainties, the branching ratio is found to be $\mathcal{B}(B \to \tau\nu) = (0.96 \pm 0.26) \times 10^{-4}$ with a significance of 4.0σ [6].

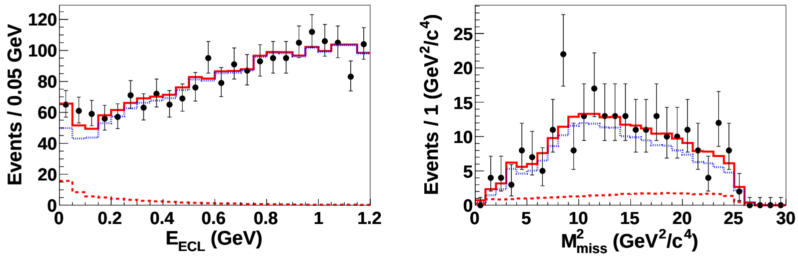

Figure 1: Signal extraction for $B \to \tau\nu$ in the latest Belle analysis [6]. Two-dimensional fit to residual energy E_{ECL} (left) and missing mass squared M_{miss} (right) is used. M_{miss} distribution is shown for a signal region of $E_{ECL} < 0.2\,\text{GeV}$. Solid circles with error bars represent data. Solid histograms show projections of the fits, dashed and dotted histograms show signal and background components, respectively.

The BaBar collaboration also reported the results of $B \to \tau\nu$ using hadronic and semileptonic tags. Using semileptonic tag and a data sample corresponding to 459×10^6 $B\bar{B}$ events, the branching ratio is obtained to be $\mathcal{B}(B \to \tau\nu) = [1.7 \pm 0.8(stat) \pm 0.2(syst)] \times 10^{-4}$ [8]. An evidence for $B \to \tau\nu$ is obtained with a significance of 3.8σ using hadronic tag and a data sample corresponding to 468×10^6 $B\bar{B}$ events [9]. The branching ratio is obtained to be $\mathcal{B}(B \to \tau\nu) = [1.83^{+0.53}_{-0.49}(stat) \pm 0.24(syst)] \times 10^{-4}$. Combining the two results, the branching ratio is found to be $\mathcal{B}(B \to \tau\nu) = (1.79 \pm 0.48) \times 10^{-4}$, where both statistical and systematic errors are combined in quadrature [9].

A world average for $B \to \tau\nu$ branching ratio is calculated to be $\mathcal{B}(B \to \tau\nu)_{WA} = (1.15 \pm 0.23) \times 10^{-4}$. For this calculation, the correlation in the systematic errors between the Belle and BaBar results was neglected since the statistical errors are dominant and the correlated parts in the systematic errors are relatively small. In the SM an estimate of $\mathcal{B}(B \to \tau\nu)_{SM} = (0.73^{+0.12}_{-0.07}) \times 10^{-4}$ is obtained by using f_B and $|V_{ub}|$ provided by a global fit to the CKM matrix elements [10]. The deviation is found to be 1.6σ.

In the Type II 2HDM [1], the branching ratio of $B \to \tau\nu$ is described by $\mathcal{B}(B \to \tau\nu) = \mathcal{B}(B \to \tau\nu)_{SM} \times r_H$, where $\mathcal{B}(B \to \tau\nu)_{SM}$ is the SM value of the branching ratio, r_H is a modification factor $r_H = (1 - \tan^2\beta\, m^2_{B^\pm}/m_{H^\pm}{}^2)^2$, $m_{B^\pm}$ is the charged B meson mass, $m_{H^\pm}$ is the charged Higgs mass and $\tan\beta$ is the ratio of the two Higgs bosons vacuum expectation values. Conservatively using $f_B = (191 \pm 9)\,\text{MeV}$ from the lattice calculation provided by the HPQCD collaboration [11] and $|V_{ub}| = (4.15 \pm 0.49) \times 10^{-3}$ from the $b \to u$ transitions provided by the PDG group [12], we evaluate excluded regions in the $\tan\beta - m_{H^\pm}$ plane as shown in Fig. 4 (left). Stringent constraint is obtained for relatively higher $\tan\beta$ region.

1.3 $B \to \ell\nu$

In Type 2 II 2HDM branching ratios of all leptonic B decays are modified by the same factor r_H and it is interesting to measure $B \to \ell\nu$ decays in addition to $B \to \tau\nu$ decay. The highly suppressed $B \to \ell\nu$, $\ell = e, \mu$ final states are predicted to have SM branching fractions of $\mathcal{O}(10^{-11})$ and $\mathcal{O}(10^{-7})$ for $\ell = e$ and $\ell = \mu$, respectively. As these decays are two-body decays, the charged lepton momentum in the rest frame of the decaying $B_{\rm sig}$ is $p_\ell^B \simeq m_B/2$. This gives a unique signature which can be exploited in this analysis because the $B_{\rm sig}$ rest frame is known from the hadronic tagging. Most backgrounds are not expected to produce high momentum leptons that can reach the signal region, defined as $2.6\,{\rm GeV}/c < p_\ell^B < 2.7\,{\rm GeV}/c$. In the analysis using full Belle data sample of 772×10^6 $B\bar{B}$ events no events are observed in the signal region, as shown in Fig. 2, and 90% C.L. upper limits on the branching fractions are determined: $\mathcal{B}(B \to e\nu) < 3.5 \times 10^{-6}$ and $\mathcal{B}(B \to \mu\nu) < 2.5 \times 10^{-6}$ [13]. These are the most stringent limits on $B \to \ell\nu$ decays using a hadronic tag method. Previous results from Belle and BaBar using a loose tagging method (*i.e.* tracks and photons excluding the signal lepton have to be compatible with the recoiling B meson) are $\mathcal{B}(B \to e\nu) < 0.98 \times 10^{-6}$ [14] and $\mathcal{B}(B \to \mu\nu) < 1.0 \times 10^{-6}$ [15], respectively.

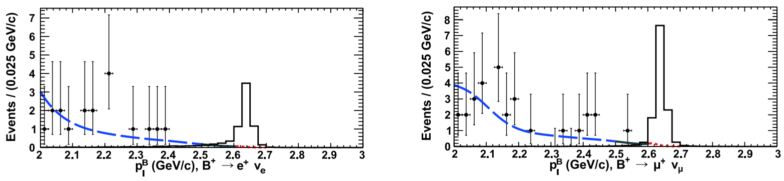

Figure 2: Results of the fit to the p_ℓ^B spectrum for $B \to e\nu$ (left) and $B \to \mu\nu$ (right) decays. Data is shown as points with error bars. The solid histogram shows the expected signal shape with arbitrary normalization. The sum of PDFs is shown as a dashed line in the sideband region ($2.0\,{\rm GeV} < p_\ell^B < 2.5\,{\rm GeV}$), where the normalization was obtained. In the signal region ($2.6\,{\rm GeV} < p_\ell^B < 2.7\,{\rm GeV}$) the sum of PDFs is shown as a dotted line.

1.4 $B \to D^{(*)}\tau\nu$

The semileptonic $B \to D^{(*)}\tau\nu$ decays also include multiple neutrinos in the final states considering the following τ decays. The results shown up to now are based on the tags using hadronic B decays. The ratios $R(D^{(*)}) = \mathcal{B}(B \to D^{(*)}\tau\nu)/\mathcal{B}(B \to D^{(*)}\ell\nu)$, which are independent of the CKM element $|V_{cb}|$ and of the parameterization of the strong interaction to a large extent, are measured. With larger statistics, the q^2 distributions and the angular distributions of the τ and $D^{(*)}$ decays could also provide useful information for testing the SM and constraining new physics models.

The $B^0 \to D^{*+}\tau^-\nu_\tau$ decay was first observed by the Belle collaboration using the 535×10^6 $B\bar{B}$ data sample [16]. The Belle collaboration also obtained the results for the charged B meson decays to $D^{(*)}\tau\nu$ using the 657×10^6 $B\bar{B}$ data sample [17]. These measurements are done by inclusively reconstructing the $B_{\rm tag}$ candidates using all the remaining particles after selecting the $B_{\rm sig}$ decay products. The Belle collaboration also obtained a preliminary result by exclusively reconstructing the $B_{\rm tag}$ candidates and the $B_{\rm sig}$ decay products using the 657×10^6 $B\bar{B}$ data sample [18]. Figure 3 shows the distributions of the kinematic variables used for the signal extraction. The naive averages of $R(D^{(*)})$ for the above results are obtained to be $R(D) = 0.430 \pm 0.091$ and $R(D^*) = 0.405 \pm 0.047$ [19]. For the calculation, the correlations in the statistical errors between the different tagging analyses are neglected since the event overlap is very limited. The correlations in the systematic errors between the different tagging analyses are assumed to be 60%.

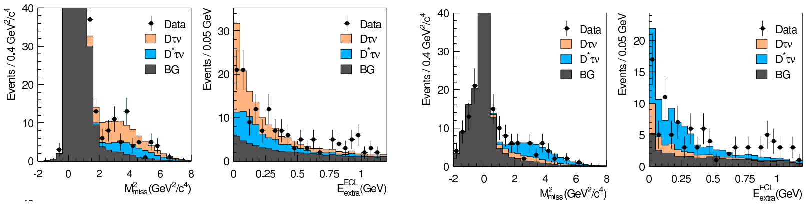

Figure 3: Signal extraction for $B \to D^{(*)}\tau\nu$ in Belle analysis [18] is shown for $B^+ \to \bar{D}^0\tau^+\nu$ (two left plots) and $B^+ \to \bar{D}^{*0}\tau^+\nu$ (two right plots). The missing mass squared M^2_{miss} and residual energy E^{ECL}_{extra} are used.

The BaBar collaboration showed the latest results for the $B \to D^{(*)}\tau\nu$ decays using hadronic tag and the full 471×10^6 $B\bar{B}$ data sample [20]. This analysis includes a signal efficiency increase by more than a factor of three compared to the previous analysis [21]. This improvement is provided by adding more $B_{\rm tag}$ decay chains and using a looser charged lepton selection. The background events are subtracted by employing the boosted decision tree multivariate method. Combining the results for the neutral and charged B decays to $D^{(*)}\tau\nu$, the $R(D^{(*)})$ ratios are obtained to be $R(D) = 0.440 \pm 0.058(stat) \pm 0.042(syst)$ and $R(D^*) = 0.332 \pm 0.024(stat) \pm 0.018(syst)$. A negative correlation of -0.27 between $R(D)$ and $R(D^*)$ is obtained including systematic uncertainties.

The results of $R(D^{(*)})$ are consistent between the Belle and BaBar experiments. The Belle results exceed the SM predictions $R(D)_{SM} = 0.297 \pm 0.017$ and $R(D^*)_{SM} = 0.252 \pm 0.003$ [22] by 1.4σ and 3.0σ, respectively [19]. The BaBar results exceed these SM predictions by 2.0σ and 2.7σ, respectively [20]. The combined disagreement of the discrepancy is at 4σ level [19].

In the Type II 2HDM, there is a substantial impact on the ratios $R(D^{(*)})$ due to the charged Higgs contribution [23]. The result for Belle, shown in Fig. 4 (right) has been obtained privately by ignoring the correlation between the experimental $R(D)$ and $R(D^{(*)})$ results and the dependency of the experimental $R(D^{(*)})$ results on $m_{H^\pm}$ and $\tan\beta$. The BaBar result includes both of them [20]. Both results disfavor the Type II 2HDM by a level of more than 3σ for all $\tan\beta/m_{H^\pm}$ region.

1.5 Summary

Exploiting the large number of events and the clean environment at the B-factories, the leptonic $B \to \tau\nu$ and the semileptonic $B \to D^{(*)}\tau\nu$ decays were measured with a good precision in spite of the existence of multiple neutrinos in the final states. Upper limits were set for the highly suppressed leptonic $B \to \ell\nu$, $\ell = e, \mu$ decays. Stringent constraints on the charged Higgs mass $m_{H^\pm}$ and the vacuum-expectation-value ratio $\tan\beta$ were evaluated for the Type II 2HDM. Further investigation at the next-generation B-factories is important for testing the SM and for constraining new physics models.

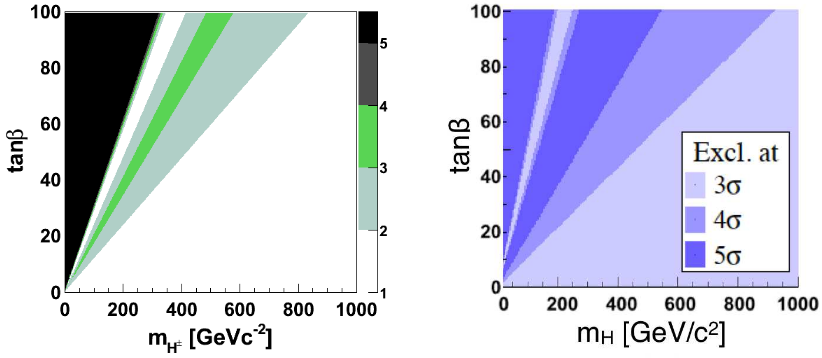

Figure 4: Constraint on $\tan\beta$ and $m_{H^\pm}$ in the Type II 2HDM obtained from Belle results, from measured $\mathcal{B}(B \to \tau\nu)$ (left) and $R(^{D^{(*)}})$ values (right).

2 Bottomonium study

2.1 Observation of Z_b states in the $\Upsilon(nS)\pi^+\pi^-$ and $h_b(mP)\pi^+\pi^-$ channels

Recently Belle observed the $h_b(1P)$ and $h_b(2P)$ states in the transitions $\Upsilon(5S) \to h_b(mP)\pi^+\pi^-$ [24]. The rates of these transitions appeared to be unsuppressed relative to the $\Upsilon(5S) \to \Upsilon(nS)\pi^+\pi^-$ $(n = 1, 2, 3)$. The $h_b(mP)$ production involves spin-flip of b-quark and is suppressed as $(\Lambda_{QCD}/m_b)^2$ in the multipole expansion; this unexpected result motivated further studies of the $h_b(mP)$ and $\Upsilon(nS)$ production mechanisms.

Belle studied the resonant structure of the $\Upsilon(5S) \to \Upsilon(nS)\pi^+\pi^-$ and $h_b(mP)\pi^+\pi^-$ decays $(n = 1, 2, 3;\ m = 1, 2)$ [25]. The $\Upsilon(nS)$ [$h_b(mP)$] states are reconstructed in the $\mu^+\mu^-$ channel [inclusively using missing mass of the $\pi^+\pi^-$ pairs]. Invariant mass spectra of the $\Upsilon(nS)\pi^\pm$ and $h_b(mP)\pi^\pm$ combinations are shown in Fig. 5. Each distribution shows two peaks. For the channels $\Upsilon(nS)\pi^+\pi^-$ [$h_b(mP)\pi^+\pi^-$] the Dalitz plot analysis [fit to one-dimensional distributions] is performed. The non-resonant contributions in the $h_b(mP)\pi^+\pi^-$ channels are negligible, justifying the one-dimensional analysis. Preliminary results of the angular analysis indicate that both states have the same spin-parity $J^P = 1^+$ [26], therefore coherent sum of Breit-Wigner amplitudes is used to describe the signals. The Dalitz plot model for the $\Upsilon(5S) \to \Upsilon(nS)\pi^+\pi^-$ channels includes also the $\pi^+\pi^-$ resonances $f_0(980)$ and $f_2(1270)$, and non-resonant contribution, parameterized as $a + b\,M^2_{\pi^+\pi^-}$, where a and b are complex numbers floating in the fit. The masses and widths of the two peaks are found to be in good agreement among different channels.Averaged over the five decay channels parameters are $M_1 = (10607.4 \pm 2.0)\,\mathrm{MeV}/c^2$, $\Gamma_1 = (18.4 \pm 2.4)\,\mathrm{MeV}$, $M_2 = (10652.2 \pm 1.5)\,\mathrm{MeV}/c^2$, $\Gamma_2 = (11.5 \pm 2.2)\,\mathrm{MeV}$. The peaks are identified as signals of two new states, named $Z_b(10610)$ and $Z_b(10650)$.

Another result of the amplitude analyses is that the phase between the $Z_b(10610)$ and $Z_b(10650)$ amplitudes is zero for the $\Upsilon(nS)\pi^+\pi^-$ channels, and 180° for the $h_b(mP)$ channels.

The masses of the $Z_b(10610)$ and $Z_b(10650)$ states are close to the $B\bar{B}^*$ and $B^*\bar{B}^*$ thresholds, respectively. All the properties of the $Z_b(10610)$ and $Z_b(10650)$ find natural explanation once molecular structure for these states is assumed without even the need of dynamic model.

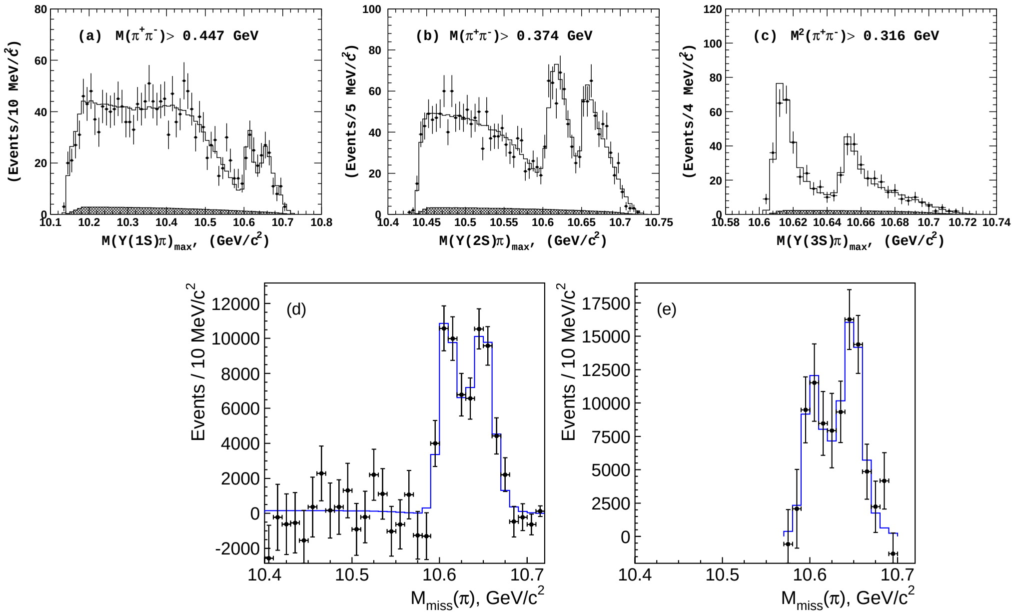

Figure 5: Invariant mass spectra of the (a) $\Upsilon(1S)\pi^{\pm}$, (b) $\Upsilon(2S)\pi^{\pm}$, (c) $\Upsilon(3S)\pi^{\pm}$, (d) $h_b(1P)\pi^{\pm}$ and (e) $h_b(2P)\pi^{\pm}$ combinations.

Considering the heavy-quark spin structure of the $B^{(*)}\bar{B}^*$ molecule with $I^G(J^P) = 1^+(1^+)$, one concludes that Z_b contain both ortho- and para-bottomonium components [27]. The weight of these components is equal, therefore the decay to the $h_b(mP)\pi^{\pm}$ is not suppressed relative to the $\Upsilon(nS)\pi^{\pm}$. The $Z_b(10610)$ and $Z_b(10650)$ differ by the sign between ortho- and para-bottomonium components, this explains why the $Z_b(10610)$ and $Z_b(10650)$ amplitudes appear with the sign plus for the $\Upsilon(nS)\pi^+\pi^-$ channels and with the sign minus for the $h_b(mP)\pi^+\pi^-$ channels. In the limit of infinitely heavy b quark the B and B^* mesons have equal mass, thus the $Z_b(10610)$ and $Z_b(10650)$ are also degenerate. Given minus sign between the Z_b amplitudes in the $h_b(mP)\pi^+\pi^-$ channel the contribution of this channel vanishes if the heavy quark symmetry is exact.

2.2 Observation of the $Z_b(10610) \to B\bar{B}^*$ and $Z_b(10650) \to B^*\bar{B}^*$ decays

Given proximity to the thresholds and finite widths, it is natural to expect that the rates of the "fall-apart" decays $Z_b(10610) \to B\bar{B}^*$ and $Z_b(10650) \to B^*\bar{B}^*$ are substantial in the molecular picture. To search for these transitions Belle studied the $\Upsilon(5S) \to [B^{(*)}\bar{B}^*]^{\pm}\pi^{\mp}$ decays [28]. One B meson is reconstructed fully using the $D^{(*)}\pi^+$ and $J/\psi K^{(*)}$ channels. The distribution of the missing mass of the $B\pi^{\pm}$ pairs shows clear signals of the $\Upsilon(5S) \to [B\bar{B}^*]^{\pm}\pi^{\mp}$ and $\Upsilon(5S) \to [B^*\bar{B}^*]^{\pm}\pi^{\mp}$ decays [see Fig. 6 (a)]; corresponding branching fractions of $(2.83 \pm 0.29 \pm 0.46)$ % and $(1.41 \pm 0.19 \pm 0.24)$ %, respectively, are in agreement with previous Belle measurement [29]. No signal of the $\Upsilon(5S) \to [B\bar{B}]^{\pm}\pi^{\mp}$ decay is found, with upper limit on its fraction of < 0.4 % at 90% confidence level.

The distributions in the $B\bar{B}^*$ and $B^*\bar{B}^*$ invariant mass for the $\Upsilon(5S) \to [B\bar{B}^*]^{\pm}\pi^{\mp}$ and

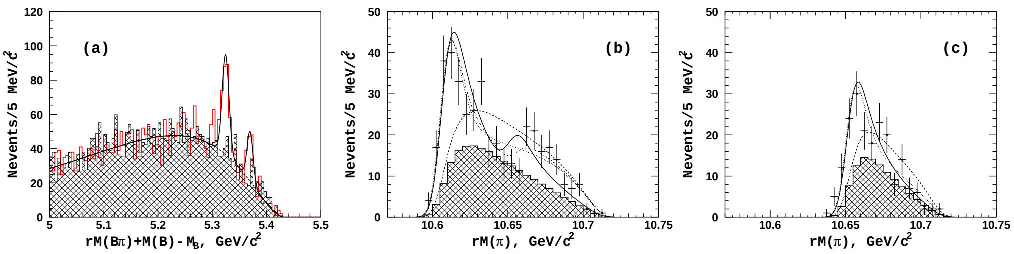

Figure 6: Missing mass of the pairs formed from the reconstructed B candidate and charged pion (a) and missing mass of the charged pions for the $B\pi$ combinations for (b) $\Upsilon(5S) \to B\bar{B}^*\pi$ and (c) $\Upsilon(5S) \to B^*\bar{B}^*\pi$ candidate events.

$\Upsilon(5S) \to [B^*\bar{B}^*]^{\pm}\pi^{\mp}$ signal regions, respectively, indicate clear excess of events over background, peaking at the thresholds [see Fig. 6 (b) and (c)]. These threshold peaks are interpreted as the signals of the $Z_b(10610) \to B\bar{B}^*$ and $Z_b(10650) \to B^*\bar{B}^*$ decays, with significances of $8\,\sigma$ and $6.8\,\sigma$, respectively. Despite much larger phase-space, no significant signal of the $Z_b(10650) \to B\bar{B}^*$ decay is found.

Assuming that the Z_b decays are saturated by the channels so far observed, Belle calculated relative branching fractions of the $Z_b(10610)$ and $Z_b(10650)$ (see Table 1). The $B^{(*)}\bar{B}^*$ channel is dominant and accounts for about 80% of the Z_b decays. The $Z_b(10650) \to B\bar{B}^*$ channel is not included in the table because its significance is marginal. If considered, the $Z_b(10650) \to B\bar{B}^*$ branching fraction would be $(25.4 \pm 10.2)\%$. All other fractions would be reduced by a factor of 1.33.

Table 1: Branching fractions ($\mathcal{B}$) of $Z_b(10610)$ and $Z_b(10650)$ assuming that the observed so far channels saturate their decays.

Channel	$\mathcal{B}$ of $Z_b(10610)$, %	$\mathcal{B}$ of $Z_b(10650)$, %
$\Upsilon(1S)\pi^+$	0.32 ± 0.09	0.24 ± 0.07
$\Upsilon(2S)\pi^+$	4.38 ± 1.21	2.40 ± 0.63
$\Upsilon(3S)\pi^+$	2.15 ± 0.56	1.64 ± 0.40
$h_b(1P)\pi^+$	2.81 ± 1.10	7.43 ± 2.70
$h_b(2P)\pi^+$	2.15 ± 0.56	14.8 ± 6.22
$B^+\bar{B}^{*0} + \bar{B}^0 B^{*+}$	86.0 ± 3.6	–
$B^{*+}\bar{B}^{*0}$	–	73.4 ± 7.0

2.3 Evidence for neutral isotriplet member $Z_b(10610)^0$

Both $Z_b(10610)$ and $Z_b(10650)$ are isotriplets with only charged components observed originally. Belle searched for their neutral components using the $\Upsilon(5S) \to \Upsilon(nS)\pi^0\pi^0$ ($n = 1, 2$) decays [30]. These decays are observed for the first time and the measured branching fractions $\mathcal{B}[\Upsilon(5S) \to \Upsilon(1S)\pi^0\pi^0] = (2.25 \pm 0.11 \pm 0.22) \times 10^{-3}$ and $\mathcal{B}[\Upsilon(5S) \to \Upsilon(2S)\pi^0\pi^0] = (3.66 \pm 0.22 \pm 0.48) \times 10^{-3}$, are in agreement with isospin relations.

Belle performed the Dalitz plot analyses of the $\Upsilon(5S) \to \Upsilon(1S, 2S)\pi^0\pi^0$ transitions using the same model as for the charged pion channels (see Fig. 7). The $Z_b(10610)^0$ signal is found

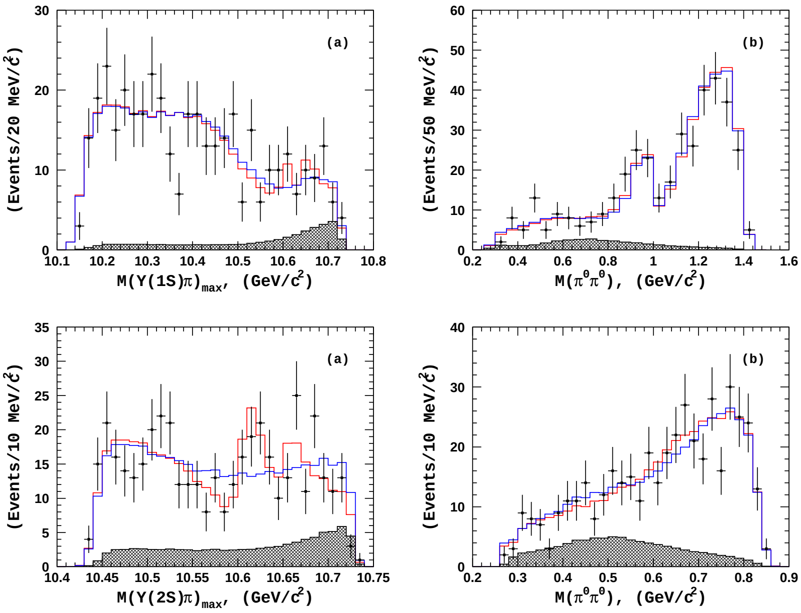

Figure 7: The projections of the Dalitz plot fit for the $\Upsilon(1S)\pi^0\pi^0p$ (top row) and $\Upsilon(2S)\pi^0\pi^0$ (bottom row) channels on the $\Upsilon(nS)\pi^0$ (left column) and $\pi^0\pi^0$ invariant mass.

in the $\Upsilon(2S)\pi^0$ channel with the significance of $4.9\,\sigma$ including systematics. The $Z_b(10610)^0$ mass of $(10609^{+8}_{-6} \pm 6)\,\text{MeV}/c^2$ is consistent with the charged $Z_b(10610)^{\pm}$ mass. The signal of the $Z_b(10610)^0$ in the $\Upsilon(1S)\pi^0$ channel and the $Z_b(10650)^0$ signal are insignificant. The Belle data do not contradict the existence of the $Z_b(10610)^0 \to \Upsilon(1S)\pi^0$ and the $Z_b(10650)^0$, but the available statistics are insufficient to establish these signals.

2.4 Interpretations

As discussed at the end of Section 2.2, the assumption of molecular $B^{(*)}\bar{B}^*$ structure naturally explains all observed so far properties of the Z_b states. Their dynamical model, however, is an open question. Proposed interpretations include presence of the compact tetraquark [31], non-resonant rescattering [32], multiple rescatterings that result in the amplitude pole known as coupled channel resonance [33] and deutron-like molecule bound by meson exchanges [34]. All these mechanisms (except for the tetraquark) are intimately related and correspond rather to quantitative than to qualitative differences. Further experimental and theoretical studies are needed to clarify the nature of the Z_b states.

As discussed in Ref. [27], based on heavy quark symmetry one can expect more states with similar nature but with differing quantum numbers. Such states should be accessible in radiative and hadronic transitions in data samples with high statistics at and above the $\Upsilon(5S)$, that will be available at the SuperKEKB.

2.5 Summary

Despite observed only recently, the Z_b states provide a very rich phenomenological object with a lot of experimental information available. They could be very useful for understanding dynamics of the hadronic systems near and above the open flavor thresholds.

3 CKM measurements

Violation of the combined charge-parity symmetry (CP violation) in the SM arises from a single irreducible complex phase in the Cabibbo-Kobayashi-Maskawa (CKM) quark-mixing matrix [35, 36]. Decays that proceed dominantly through the $\bar{b} \to \bar{u}u\bar{d}$ transition are sensitive to the interior angle of the unitarity triangle $\phi_2\,(\alpha) \equiv \arg(-V_{td}V_{tb}^*)/(V_{ud}V_{ub}^*)$. A feature common to these measurements is that possible loop contributions, in addition to the leading order tree amplitude, can shift the measured angle to $\phi_2^{\text{eff}} \equiv \phi_2 + \Delta\phi_2$. Fortunately, this inconvenience can be overcome with bounds on $\Delta\phi_2$ determined using either an isospin analysis [37] or $SU(3)$ flavor symmetry [38].

Recently Belle published two papers concerning study of $B^0 \to \pi^+\pi^-$ [39] and $B^0 \to \rho^0\rho^0$ [40] decays. Both analyses used the final Belle data sample containing 772×10^6 $B\bar{B}$ pairs collected at the $\Upsilon(4S)$ resonance.

In $B^0 \to \pi^+\pi^-$ decay analysis an improved measurement of the CP violation parameters was performed, which yielded $\mathcal{A}_{CP}(B^0 \to \pi^+\pi^-) = +0.33 \pm 0.06$ (stat) $\pm$ 0.03 (syst) and $\mathcal{S}_{CP}(B^0 \to \pi^+\pi^-) = -0.64 \pm 0.08$ (stat)$\pm$0.03 (syst), confirming CP violation in these channels reported in previous measurements and other experiments. These results from the full Belle data sample after reprocessing with a new tracking algorithm and with an optimized analysis performed with a single simultaneous fit, supersede those of the previous Belle analysis [41]. They are now the world's most precise measurement of time-dependent CP violation parameters in $B^0 \to \pi^+\pi^-$, ruling out the range $23.8^\circ < \phi_2 < 66.8^\circ$, at the 1σ level.

Since the dominant tree process in $B^0 \to \rho^0\rho^0$ is color-suppressed, it is expected to be rarer than its isospin partners, making the isospin analysis less ambiguous. The vector state $\rho^0\rho^0$ is not a pure CP eigenstate, but rather a superposition of CP-even and -odd states, or three helicity amplitudes, with only the longitudinal one being a pure CP eigenstate. In general, the different helicity amplitudes can be separated through an angular analysis. This analysis is concerned with the branching fraction of $B^0 \to \rho^0\rho^0$ decays, the fraction of longitudinal polarization in these decays and decays into four charged pion final states as the ρ^0 decays dominantly into two charged pions.

Branching fraction was measured to be $\mathcal{B}(B^0 \to \rho^0\rho^0) = (1.02 \pm 0.30\text{ (stat)} \pm 0.22\text{ (syst)}) \times 10^{-6}$ with a longitudinally polarization fraction $f_L = 0.21^{+0.18}_{-0.22}$ (stat)$\pm$0.11 (syst). The branching fraction's upper limit is $\mathcal{B}(B^0 \to \rho^0\rho^0) < 1.5 \times 10^{-6}$ at 90% confidence level. The longitudinal polarization fraction was used to determine the CKM matrix angle $\phi_2 = (91.0 \pm 7.2)^\circ$ through an isospin analysis in the $B \to \rho\rho$ system. Furthermore for possible decays with the same final state the following branching fractions were obtained: $\mathcal{B}(B^0 \to f_0\rho^0) \times \mathcal{B}(f_0 \to \pi^+\pi^-) = (0.86 \pm 0.27\text{ (stat)} \pm 0.15\text{ (syst)}) \times 10^{-6}$, with a significance of 3.0 standard deviations, and upper limits at 90% confidence level on the (product) branching fractions, $\mathcal{B}(B^0 \to \pi^+\pi^-\pi^+\pi^-) < 11.7 \times 10^{-6}$, $\mathcal{B}(B^0 \to \rho^0\pi^+\pi^-) < 12.2 \times 10^{-6}$, $\mathcal{B}(B^0 \to f_0\pi^+\pi^-) \times \mathcal{B}(f_0 \to \pi^+\pi^-) < 3.1 \times 10^{-6}$ and $\mathcal{B}(B^0 \to f_0 f_0) \times \mathcal{B}(f_0 \to \pi^+\pi^-)^2 < 0.2 \times 10^{-6}$. For $B^0 \to f_0\rho^0$ decay this is the first evidence with such a significance.

References

[1] W. S. Hou, Phys. Rev. D **48**, 2342 (1993).

[2] S. Baek and Y. G. Kim, Phys. Rev. D **60**, 077701 (1999).

[3] R. Garisto, Phys. Rev. D **51**, 1107 (1995); M. Tanaka, Z. Phys. C **67**, 321 (1995).

[4] K. Ikado *et al.* (Belle Collaboration), Phys. Rev. Lett. **97**, 251802 (2006).

[5] K. Hara *et al.* (Belle Collaboration), Phys. Rev. D **82**, 071101(R) (2010).

[6] K. Hara *et al.* (Belle Collaboration), Phys. Rev. Lett. **110**, 131801 (2013).

[7] M. Feindt *et al.*, Nucl. Instrum. Meth. A **654**, 432 (2011).

[8] B. Aubert *et al.* (BaBar Collaboration), Phys. Rev. D **81**, 051101(R) (2010).

[9] J. P. Lees *et al.* (BaBar Collaboration), Phys. Rev. D **88**, 031102 (2013).

[10] J. Charles *et al.* (CKMfitter Group), Eur. Phys. J. C **41**, 1 (2005).

[11] H. Na *et al.* (HPQCD Collaboration), Phys. Rev. D **86**, 034506 (2012).

[12] J. Beringer *et al.* (Particle Data Group), Phys. Rev. D **86**, 010001 (2012).

[13] Y. Yook, PoS ICHEP2012 369 (2012).

[14] N. Satoyama *et al.* (Belle Collaboration), Phys. Lett. B **647**, 67 (2007).

[15] B. Aubert *et al.* (BaBar Collaboration), Phys. Rev. D **79**, 091101 (2009).

[16] A. Matyja *et al.* (Belle Collaboratoin), Phys. Rev. Lett. **99**, 191807 (2007).

[17] A. Bozek *et al.* (Belle Collaboration), Phys. Rev. D **82**, 072005 (2010).

[18] I. Adachi *et al.* (Belle Collaboration), arXiv:0910.4301.

[19] A. Bozek, *Summary of $B \to D^{(*)}\tau\nu$ measurements*, 2nd KEK Flavor Factory Workshop, KEK, Tsukuba, Japan (2013).

[20] J. P. Lees *et al.* (BaBar Collaboration), Phys. Rev. Lett. **109**, 101802 (2012); arXiv:1303.0571.

[21] B. Aubert *et al.* (BaBar Collaboration), Phys. Rev. Lett. **100**, 021801 (2008).

[22] S. Fajfer, J. F. Kamenik and I. Nisandzic, Phys. Rev. D **85**, 094025 (2012).

[23] M. Tanaka and R. Watanabe, Phys. Rev. D **82**, 034027 (2010); M. Tanaka and R. Watanabe, Phys. Rev. D **87**, 034028 (2013).

[24] I. Adachi *et al.* (Belle Collaboration), Phys. Rev. Lett. **108**, 032001 (2012).

[25] A. Bondar *et al.* (Belle Collaboration), Phys. Rev. Lett. **108**, 122001 (2012).

[26] I. Adachi *et al.* (Belle Collaboration), arXiv:1105.4583 [hep-ex].

[27] A. E. Bondar, A. Garmash, A. I. Milstein, R. Mizuk and M. B. Voloshin, Phys. Rev. D **84**, 054010 (2011).

[28] I. Adachi *et al.* (Belle Collaboration), arXiv:1209.6450 [hep-ex].

[29] A. Drutskoy *et al.* (Belle Collaboration), Phys. Rev. D **81**, 112003 (2010).

[30] I. Adachi *et al.* (Belle Collaboration), arXiv:1207.4345 [hep-ex].

[31] A. Ali, C. Hambrock and W. Wang, Phys. Rev. D **85**, 054011 (2012).

[32] D. -Y. Chen and X. Liu, Phys. Rev. D **84**, 094003 (2011).

[33] I. V. Danilkin, V. D. Orlovsky and Y. .A. Simonov, Phys. Rev. D **85**, 034012 (2012).

[34] S. Ohkoda, Y. Yamaguchi, S. Yasui, K. Sudoh and A. Hosaka, Phys. Rev. D **86**, 014004 (2012).

[35] N. Cabibbo, Phys. Rev. Lett. **10**, 531 (1963).

[36] M. Kobayashi and T. Maskawa, Prog. Theor. Phys. **49**, 652 (1973).

[37] M. Gronau and D. London, Phys. Rev. Lett **65**, 3381 (1990).

[38] M. Gronau and J. Zupan, Phys. Rev. D **73**, 057502 (2006).

[39] J. Dalseno *et al.* (Belle Collaboration), Phys. Rev. D **88**, 092003 (2013).

[40] P. Vanhoefer *et al.* (Belle Collaboration), arXiv:1212.4015 [hep-ex].

[41] H. Ishino *et al.* (Belle Collaboration), Phys. Rev. Lett **98**, 211801 (2007).